An Acad Bras Cienc (2024) 96(Suppl. 2): e20240581 DOI 10.1590/0001-3765202420240581
Anais da Academia Brasileira de Ciências | *Annals of the Brazilian Academy of Sciences*
Printed ISSN 0001-3765 I Online ISSN 1678-2690
www.scielo.br/aabc | www.fb.com/aabcjournal

SOIL SCIENCE

Pedodiversity and ornithogenesis of a tiny Antarctic Island (Half Moon): landform-geology-vegetation interrelationships

DANIELA SCHMITZ, RAFAEL G. SIQUEIRA, ROBERTO F.M. MICHEL, ANTONIO B. PEREIRA, JAIR PUTZKE, MARCIO R. FRANCELINO, CARLOS ERNESTO G.R. SCHAEFER

Abstract: The harsh Antarctic climate limits soil formation and the development of terrestrial ecosystems, with most biological activity concentrated in the short summer season in ice-free areas. There, penguins play a crucial role in nutrient transport from marine to terrestrial environments, significantly impacting soil properties through guano deposition. This study focuses on characterizing the ornithogenic soils of Half Moon Island in Maritime Antarctica, examining how lithology, vegetation, and geomorphology influence their formation and distribution. Fieldwork conducted during the 2014/2015 austral summer included excavating and sampling 21 soil profiles. Soils were analyzed for physical and chemical properties and classified. Half Moon Island's soils are predominantly Cryosols and Leptosols, characterized by little development, high gravel content (skeletic), and significant cryoturbation. High variability in soil chemical properties was observed, with principal component analysis highlighting distinct clusters based on landscape position, geology, vegetation and ornithogenic influence. The findings underscore the diverse pedoenvironments of Half Moon Island, shaped by past and present ornithogenic activity and post-glacial geomorphological processes. This research highlights the soil variability in Antarctic environments and the significant ecological importance of seabird colonies on small, isolated islands.

Key words: climate change, cryosols, pedogenesis, phosphatization.

INTRODUCTION

The harsh climate of Antarctica restricts soil genesis and the development of life forms in terrestrial environments (Campbell & Claridge 1987). Biological activity is restricted to short summers and ice-free areas, limited to islands, coastal regions, cliffs, and exposed ridges (Convey et al. 2008). Coastal stretches emerged after the Last Glacial Maximum (LGM), during global Holocene deglaciation (10 ka), and subsequent glacial-isostatic land uplift, increased the area accessible to marine vertebrates, particularly penguins and seals (Tatur 2002). This process accelerated in the last 6 ka when wide raised beaches and terraces formed at the base of early Holocene cliffs (Fretwell et al. 2010). Thus, the first marine animals breeding grounds often shifted to these seaward beaches, resulting that earlier higher sites, located on the steep Early Holocene cliffs, were abandoned (Tatur et al. 1997, Tatur 2002).

Penguins are important seabirds for the transport of nutrients from the sea to terrestrial ecosystems in Antarctica, since they form large colonies and use the same area for breeding for centuries (Santamans et al. 2017). In addition, penguins feed almost exclusively

in the marine environment, but deposit many droppings, feathers bones, and eggshells in terrestrial environments (Perfetti-Bolaño et al. 2018). According to Simas et al. (2007), guano accumulation in penguin rookeries represents the most abundant source of organic matter in the Antarctic terrestrial ecosystem, reaching 10 kg of guano per m^2 per year (Myrcha & Tatur 1991). Penguin colonies are generally located in well-drained and elevated sites, not far (maximum 350 m) from the coast and up to 60 m high in altitude (Santora et al. 2020).

Other birds (gulls, skuas, and petrels) nest in more central ice-free areas. Dense populations of penguins, giant petrels, and sea gulls entering new areas often limit the vegetation growth due to nutrient excess and toxicity. However, the vegetation around the nests of other flying birds (small petrels, Antarctic terns), or around individual skua nests is not affected, but greatly fertilized (Tatur 2002). With the abandonment and/or displacement of penguin colonies, due to climatic changes or uplift by post-LGM glacio-isostasy, the former penguin rookeries are colonized by varying cryptogamic plant communities, as the soils at these sites are very fertile (Ferrari et al. 2021, Schmitz et al. 2020).

Antarctic soils are generally poorly developed, unstable, and strongly influenced by freeze-thaw cycles; usually have low clay and organic matter contents, and high gravel and pebble contents (Convey et al. 2008, Pereira et al. 2013, Daher et al. 2019, Lopes et al. 2019). Among the main soil types in Antarctica, ornithogenic soils are characterized by their unique properties, which are directly related to the higher degree of weathering of these soils, influenced by the deposition of guano from seabirds, rich in phosphorus, nitrogen and nutrients (Michel et al. 2006, Simas et al. 2007, Poggere et al. 2016, Schaefer et al. 2017, Daher et al. 2019). Phosphatization is the most important pedogenic process in these Antarctic soils, associated with intense geochemical transformations and the precipitation of a new assembly of phosphate minerals (Rodrigues et al. 2021, Sacramento et al. 2023). The ornithogenic soils are also enriched with organic matter, especially at the abandoned sites, constituting pools of soil carbon stocks in Antarctic ecosystems (Michel et al. 2006).

The aim of this work was to present the main soils and their distribution in a tiny island (Half Moon Island - HMI), in Maritime Antarctica, aiming to understand how the substrates, geomorphology and vegetation influence the soil distribution and ornithogenesis. Our hypothesis is that HMI, despite its very small size, has a large pedological diversity that is related to the interplay of past and present ornithogenic influence, combined with landscape evolution, particularly post-LGM glacial glacio-isostatic events, and vegetation development.

MATERIALS AND METHODS

Study area

With an area of approximately 1.6 km^2, Half Moon Island (62°35'42.94" S 59°55'8.41" W) is a small island in the McFarlane Strait between Greenwich Island (to the northeast) and Livingston Island (to the southwest) (Figure 1a), which is part of the South Shetland archipelago, Maritime Antarctica. The fieldwork was conducted during the 33rd Brazilian Antarctic Operation, in the austral summer of 2014/2015. The island takes its name from its crescent moon shape. It is home to the Argentinian Camara Base, which was built in 1951/1952. The average annual air temperature on Half Moon Island ranged from -3.11 °C to -1.10 °C between 2015 and 2018, with a minimum of -17.93 °C and a maximum of 12.81 °C during this period (Schaefer et al. 2023).

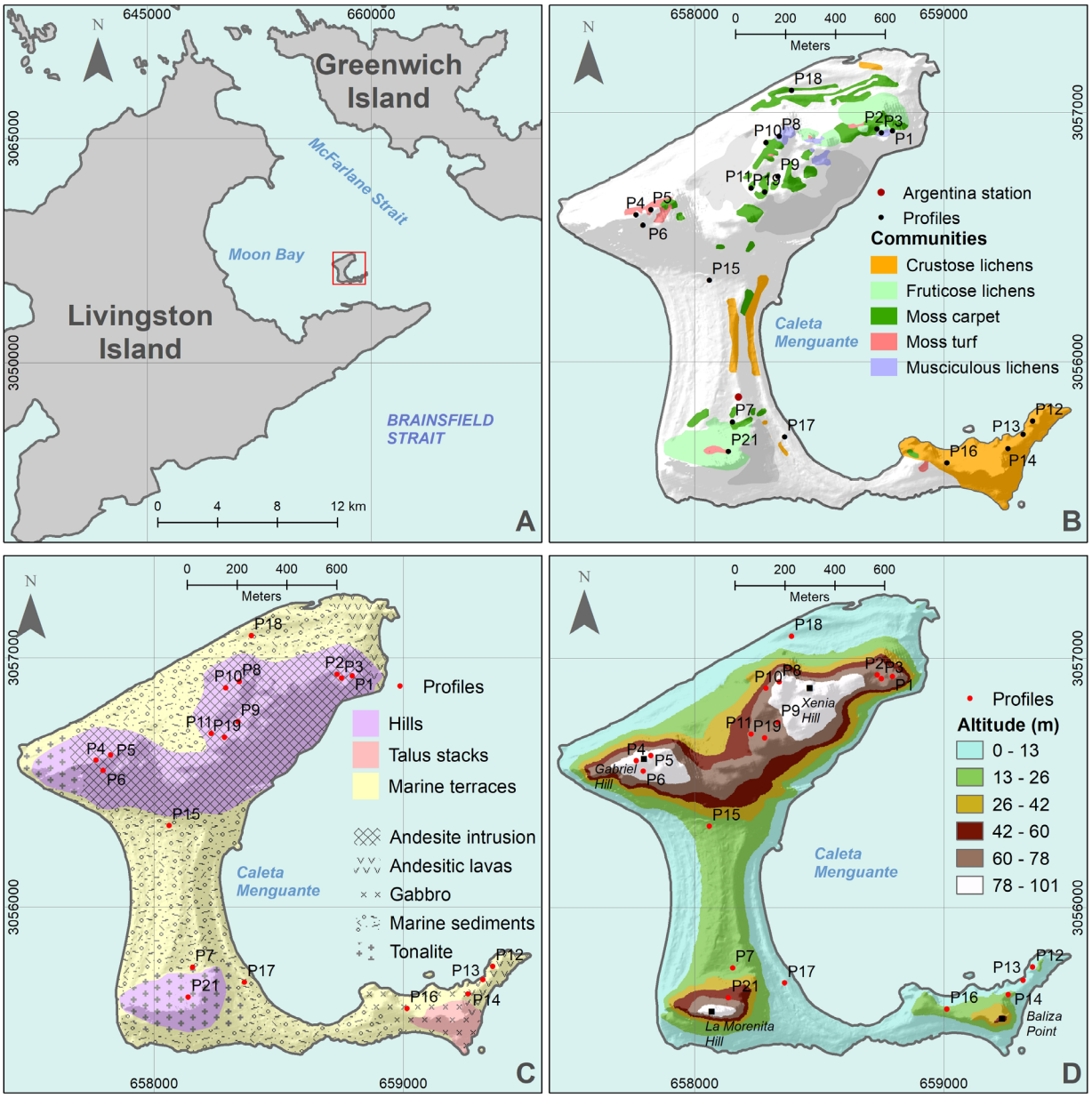

Figure 1. a) The location of Half Moon Island in McFarlane Strait, b) Plant community map with the 21 sampled profiles on Half Moon Island (adapted from Schmitz et al. 2018), c) Geological map of the island, showing the locations of the 21 sampled profiles (adapted from Smellie et al. 1984), d) Altitude map of the island, showing the locations of the 21 sampled soil profiles.

Half Moon Island possesses colonies of almost all representative Antarctic birds, in addition to colonies of seals resting in the area. Birds were counted on this island in some previous studies. According to Esponda et al. (2000), there were 10 breeding species on Half Moon Island in the Antarctic summer of 1995/96: chinstrap penguins (*Pygoscelis antarctica*), Cape petrels (*Daption capense*), Wilson's storm petrels (*Oceanites oceanicus*), black-bellied storm petrels (*Fregetta tropica*), Antarctic cormorants (*Leucocarbo bransfieldensis*), Subantarctic

skuas (*Catharacta antarctica*), South Polar skuas (*C. maccormicki*), kelp gulls (*Larus dominicanus*), Antarctic terns (*Sterna vittata*), and snowy sheathbills (*Chionis alba*).

The number of vegetation species recorded amounted to 38 bryophytes, 59 lichens, only one flowering plant (*Deschampsia antarctica* Desv.), and two macroscopic terrestrial algae (Schmitz et al. 2018). Five types of plant communities were classified on the island, covering about 12.5% of the island: fruticose lichen and moss cushion, moss carpet, muscicolous lichen, crustose lichen, and moss turf (Figure 1b) (Schmitz et al. 2018, 2021). The fruticose lichen community has the greatest coverage. The crustose lichen community was the most diverse, and the moss carpet was the community with the greatest richness. Species of the genus *Sanionia* spp were the most abundant on the island (Schmitz et al. 2018, 2021).

The landscape of Half Moon Island consists of two clear divisions. The first is the compartment of hills, which consists of the remains of uplifted marine platforms bordered by scree slopes and scarps (López-Martínez et al. 2012). The slopes are the result of intense glacial erosion of the platforms during the LGM. After deglaciation, the hills developed into small islands from the pre-Holocene which were connected by tombolos during marine accumulation in the Holocene. These tombolos gave rise to the second marine compartment of HMI, consisting mainly of highly stepped plains of marine terraces with maximum height of 18 m, that were uplifted during the successive Holocene glacio-isostatic pulses (Serrano & López-Martínez 1997).

There are three large hills on Half Moon Island. Gabriel Hill (101 m a.s.l) is the highest point followed by Xenia Hill (≈ 90 m.a.s.l) and La Morenita Hill (≈ 85m a.s.l. behind Camara Base) (Figure 1d) (Schmitz et al. 2018). Penguin colonies are concentrated on Baliza Point and are frequently visited by tourists in summer. According to Smellie et al. (1984) the geology of the island is diverse and consists of andesite intrusions in the north (Gabriel and Xenia Hills) and tonalite intrusions in the south at La Morenita Hill (Figure 1c). Gabbro also occurs in HMI at Baliza Point, where it locally intrudes andesitic lavas (Serrano & López-Martínez 1997).

The geomorphology of Half Moon Island is characterized by the predominance of coastal forms and processes. There are many raised and stepped beaches, that extend from sea level to an altitude of 18 m, as well as erosional sea platforms, that range from 18 to 90 m in height (Serrano & López-Martinez 1997).

Glacial landforms and deposits are divided in to: Ice and snow, ice scarp, cirques, till, moraine ridge and diffluence; Periglacial and nival landforms and deposits: nivation niche, patterned ground, stone stripes, cracking stone, solifluction lobes, debris slopes and debris cone; Marine landforms and deposits. Landforms changed according to elevation: between 0 and 20 m a.s.l. raised beaches, cliffs, till, glacial deposits, and debris slopes and cones were most common; between 20 and 80 m a.s.l nivation niches, patterned ground, stone stripes, gelifluction sheets, and lobes were predominant; at higher elevations debris lobes and debris talus, associated with the resistance of andesite intrusions predominated (saddleback ridge, López-Martínez et al. 2012).

Soil characterization

Twenty-one profiles distributed throughout HMI were excavated and sampled to the lithic contact or permafrost (Table I), representing different degrees of ornithogenesis and various types of vegetation cover on the island (Figure 2). The morphology of the profile was described, and samples of soil horizons were sampled according to Bockheim et al. (2006). Soils were

Table I. Location, soil classification (WRB and Soil Taxonomy), landforms, geology, ornithogenic influence, and vegetation type of the 21 soil profiles (P) sampled on Half Moon Island.

P	Elev m a.s.l.	Geographic position	Classification WRB-FAO	Soil Taxonomy	Landforms	Geology	Ornithogenic influence	Vegetation type
1	83	62°35'3.30" S 59°54'28.90"W	Turbic Leptic Umbric Skeletic Cryosol (Arenic Humic Ornithic)	Typic Psammoturbels + Lithic Umbriturbels	Upper platforms and slopes	Andesite	Former, moderate	Moss carpet
2	71	62°35'3.17" S 59°54'33.3"W	Reductaquic Leptic Skeletic Cryosol (Arenic Humic Ornithic)	Lithic Umbriturbels +Lithic Aquiturbels	Upper platforms and patterned ground	Andesite	Former very strong	Moss carpet
3	76	62°35'3.65"S 59°54'31.92"W	Turbic Leptic Umbric Skeletic Cryosol (Arenic Humic)	Lithic Umbriturbels +Lithic Aquiturbels	Upper platforms and gelifluction lobes	Andesite	No or former weak	Musciculous lichens
4	100	62°35'15.78"S 59°55'39.78"W	Turbic Leptic Cryosol (Arenic, Humic)	Typic Psammoturbels + Lithic Umbriturbels	Crest ridge	Andesite	No or former weak	Moss carpet
5	90	62°35'15.8"S 59°55'35.7" W	Turbic Leptic Cryosol (Arenic Humic Ornithic)	Typic Psammoturbels + Lithic Umbriturbels	Upper platforms and gelifluction lobes	Andesite	No or former weak	Moss turf
6	65	62°35'15.30" S 59°55'15.30"W	Turbic Leptic Cryosol (Arenic)	Lithic Umbriturbels +Lithic Aquiturbels	Stone stripes	Andesite	Former strong	Unvegetated
7	40	62°35'42.94"S 59°55'8.41"W	Turbic Leptic Umbric Cryosol (Arenic Humic)	Typical Psammoturbels + Lithic Umbriturbels	Debris slope and cone	Tonalite	Former, moderate	Moss carpet
8	90	62°35'4.70"S 59°55'0.60"W	Turbic Leptic Umbric Cryosol (Arenic Humic)	Typical Psammoturbels + Lithic Umbriturbels	Middle platforms and scarps	Andesite	No or former weak	Musciculous lichens
9	80	62°35'05.6" S 59°55'04.3"W	Turbic Reductaquic Leptic Mollic Cryosol (Arenic Humic)	Lithic Umbriturbels + Lithic Aquiturbels	Upper platforms and slopes	Andesite	No or former weak	Moss carpet
10	64	62°35'05.6" S 59°55'04.3"W	Turbic Cryosol (Dystric Arenic Ornithic)	Typic Psammoturbels + Lithic Umbriturbels	Upper platforms and slopes	Andesite	Former strong	Fruticose lichens *Usnea*
11	70	62°35'11.6" S 59°55'07.8" W	Turbic Leptic Cryosol (Arenic Humic)	Lithic Umbriturbels + Lithic Aquiturbels	Upper platforms and slopes	Andesite	Former very strong	Moss carpet

Table I. Continuation.

12	5	62°35'40.0"S 59°53'45.6"W	Skeletic Leptosol (Arenic Gelic Ornithic)	Ornithogenic Lithic Gelorthent + Lithic Gelorthent	Talus stacks	Gabbro	Current strong	Unvegetated
13	3	62°35'41.8"S 59°53'48.1"W	Eutric Skeletic Leptosol (Arenic Gelic)	Ornithogenic Typic Gelorthent + Typic Gelorthent + beach gravels	Marine terraces	Marine sediments	Current strong	Unvegetated, scarse *Prasiola crispa*
14	12	62°35'43.73"S 59°53'52.19"W	Skeletic Leptosol (Arenic Gelic Ornithic)	Ornithogenic Lithic Gelorthent + Lithic Gelorthent	Talus stacks	Gabbro with Marine sediments	Current moderate	Unvegetated
15	44	62°35'23.8"S 59°55'18.3"W	Turbic Skeletic Cryosol (Arenic Eutric Patterned)	Typic Psammoturbels + Lithic Umbriturbels	Marine terraces	Andesite with Marine sediments	Former, moderate	Unvegetated
16	5	62°35'45.8" S 59°54'08.4" W	Eutric Leptosol (arenic Gelic)	Lithic Gelorthent + Typic Gelorthent + beach gravels	Marine terraces	Tonalite with Marine sediments	Former strong	Unvegetated
17	12	62°35'43.6"S 059°54'55.1"W	Skeletic Leptosol (Arenic Gelic)	Lithic Gelorthent + Typic Gelorthent + beach gravels	Marine terraces	Marine sediments	Former strong	Unvegetated
18	3	62°34'58.70"S 59°54'57.80"W	Eutric Leptosol (Siltic Gelic)	Typic Psammoturbels + Lithic Umbriturbels	Marine terraces- Present day and Holocene beaches	Marine sediments	No or former weak	Unvegetated
19	67	62°35'12.0"S 59°55'04.0"W	Turbic Umbric Cryosol (Arenic Ornithic)	Typic Psammoturbels + Lithic Umbriturbels	Upper platforms and slopes	Andesite	No or former weak	Moss carpet
20	73	62°35'11.8"S 59°55'04.7"W	Skeletic Turbic Cryosol (Arenic)	Lithic Umbriturbels + Lithic Aquiturbels	Stone stripes	Andesite	No or former weak	Unvegetated
21	85	62°35'45.9"S 59°55'08.8"W	Turbic Leptic Umbric Skeletic Cryosol (Arenic Humic)	Typic Psammoturbels + Lithic Umbriturbels	Upper platforms and slopes	Tonalite	Current Skua	Fruticose lichens - *Usnea*

classified according to the World Reference Base for Soil Resources (IUSS Working Group WRB 2015) and the Soil Taxonomy (SSS, 2014). All soil samples were analyzed in the laboratories of the Soil Department of the Federal University of Viçosa, according to standard protocols (Teixeira et al. 2017). Regarding soil chemistry, the following parameters were evaluated: available P; exchangeable K, Ca^{2+}, Na, Mg^{2+}, Al^{3+}, Fe, Cu, Mn, Zn; exchangeable acidity (H + Al); pH (H_2O);

Figure 2. Representative soil profiles and landscapes illustrating different degrees of ornithogenesis and vegetation types: (a) current strong, unvegetated (P12); (b) current weak: unvegetated (P14, above), fruticose lichens *Usnea* community (P21, below); (c) former weak to moderate: moss turf community (P4); (d) former strong: moss carpet community (P11, above; P2, below).

organic matter (OM); bases sum (BS); effective cation exchange capacity (CECeff); potential effective cation exchange capacity (CEC_T); bases saturation percentage (PSB); Al saturation (Al_sat); and remaining phosphorus (P_rem).

Soil texture was analyzed by mechanical dispersion of < 2 mm samples in distilled water, sieving and weighting of the coarse and fine sand, and sedimentation of the silt fraction followed by siphoning of the < 2 µm fraction (Gee & Bauder 1986). The soil textural classes were determined using a soil textural chart (Sand 0.05- < 2 mm, silt 0.002- < 0.05 mm, and clay < 0.002 mm). Due to the limited sample size, physical analyses could not be carried out for all environments, so they were not included in the statistical analyses.

Soil mapping

After describing and classifying the soil profiles, the soil classes of Half Moon Island were mapped. A semi-automatic method was used for this. The first step was to automatically delineate the mapping units using the SAGA tool TPI Based Landform Classification which is included in the software QGIS (QGIS 2024) and defines relief units based on the Topographic Position Index algorithm. The use of this tool is strongly based on the assumption that the soil-landscape relationship has a decisive influence on the distribution of soils at the local scale in Antarctica (Francelino et al. 2011, Schaefer et al. 2015). The second step was to classify the created landscape units, defining simple or composite mapping units depending on the distribution of soil profiles used as reference.

Statistical Analyses

The chemical soil properties were summarized using a principal component analysis (PCA) of the correlation matrix with the 'FactoMineR' package (Husson et al. 2017). This analysis aimed to reduce the number of redundant soil properties and identify patterns of similarity for four parameters: landscape units, geology, vegetation, and ornithogenesis. All analyses were performed using R software (version 4.4.0) (R Core Team 2023).

RESULTS

General soil characteristics

The soils of Half Moon Island were shallow skeletal (gravelly, cobbly, and dominated by coarse grain) and poorly developed. Soil structure ranged from moderate to weak, subangular to granular structure, or single grain. Granular structures occurred on gabbro and tonalite intrusions, while the subangular structure and single grain were related to andesite and andesitic lavas and lapilli stones, the former being closely associated with higher organic matter content and cryoturbation processes. The 21 pedons could be classified as Cryosols and Leptosols based on the presence of permafrost, continuous lithic contact within 25 cm depth, or less than 20% fine earth (by volume) (Table I). The soils were mostly arenic, and cryoturbated; organic matter and buried ornithogenic horizons were common.

These cryosols could be classified as turbic, leptic, skeletic, and, most frequently, reductaquic umbric or mollic (P1, P2, P3, P4, P5, P6, P7, P8, P9, P10, P11, P15, P19 and P21). Summer temperatures close to 0 °C were detected, together with cryoturbation during sampling, and the location in the landscape and periglacial features confirms the presence of permafrost (IUSS Working Group WRB 2015). These cryosols were located at the top of Tombolo, which connects the two rock promontories, at the highest parts of the landscape: Gabriel Hill, Xenia Hill, and La Morenita Hill. They occurred at sites dominated by periglacial and nival landforms and deposits. Leptosols (gelic) were all skeletic, often with arenic and ornithic characteristics (P12, P13, P14, P16, P17, P18 and P20); they occurred mainly on present-day and Holocene beaches at the coastal zone, always below 20 m a.s.l., with the main landforms including tills, stone stripes, and rock glaciers. Soils formed from andesite intrusions and andesitic lavas as well as lapilli stones and tonalite tended to be coarser, while those formed from gabbro intrusions have a higher silt content.

The chemical properties of the soil greatly varied in the 21 areas (Table II). Many areas showed strong ornithogenic influence (including the pedons at higher elevations) and had high acidity and very high available P values (183 to 8483 mg/dm³), with the exception of environments 15 (P= 64.1 mg/dm³) and 18 (P= 135.7 mg/dm³), which had a very low ornithogenic influence (Table II). P10 had high values for several attributes, including P, Ca, Mg, BS, and t, and the lowest for Zn (0.64 mg/dm³). P11 had the greatest variation in phosphorus (P) between horizons, with a significant increase in depth (183 to 9638 mg/dm^3). P12, located in the current penguin rookery, showed elevated levels of P (median = 8.368 mg/dm^3), potassium (K = ~3487 mg/dm^3) and sodium (Na median = 4176 mg/dm^3) in all horizons, along with the lowest organic matter (OM) content (~0.1 dag/kg). P14 is located near an active penguin rookery and had low values for K, Ca^{2+}, Mg^{2+}, BS, and CECeff, probably due to intense leaching by acidification, in contrast to high value of Zn (9.33 mg/dm³). P16 had the most acidic soil, with the lowest pH (3.7) and the highest H + Al value (43.7) a depth of 15-20 cm. The organic matter

Table II. Chemical and physical soil properties of the 21 soil profiles sampled in Half Moon Island. Where the chemical properties are: phosphor (P), potassium (K), sodium (Na), calcium (Ca^{2+}), magnesium (Mg^{2+}), aluminum (Al^{3+}), exchangeable acidity (H + Al), bases sum (BS), percentage of bases, effective cation exchange capacity (CTCeff), (CECT), percentage of bases saturation (PSB), Aluminum saturation index (Al sat), organic matter (OM), copper (Cu), manganese (Mn), iron (Fe) and zinc (Zn); and the physical properties: sand, silt and clay.

Horizon	Depth (cm)	pH		P	K	Na	Ca^{2+}	Mg^{2+}	Al^{+3}	H + Al	BS	CECeff	CECT	PSB	Al sat	OM	P-Rem	Cu	Mn	Fe	Zn	Sand	Silt	Clay	Texture
		H_2O	KCl	-------- mg/dm^3--------			----------$cmol_c/kg$----------							%		dag/kg	mg/L	mg/dm^3				%			
P1 – Turbic Leptic Umbric Skeletic Cryosol (Arenic Humic Ornithic)																									
A	0-10	4.9	4.1	399.6	109	1564.9	1.4	0.4	2.0	14.5	8.9	10.9	23.4	38.1	18.7	15.6	10.2	3.3	6.6	736.2	1.7	95	3	2	Sand
B	10-20	4.9	4.2	550.5	101	151.1	1.3	0.3	2.0	16.9	2.5	4.6	19.4	13.1	44.6	13.6	7.1	7.4	12	769	5.7	95	2	3	Sand
AE1	0-10	5.0	4.7	729.0	170	165.9	2.5	1.0	0.9	19.5	4.7	5.7	24.2	19.5	17.2	24.7	24.3	2.2	4.6	407.8	3.4	92	4	4	Sand
P2 – Reductaquic Leptic Skeletic Cryosol (Arenic Humic Ornithic)																									
O	0-20	6.4	5.7	711.8	211	85.9	3.6	0.7	0	16.9	2.8	2.8	19.7	14.2	0	21.7	9.5	3.3	16.4	517.3	0.8				
AE	0-10	5.9	4.2	6976.0	283	485.2	8.0	1.6	1.5	40.2	12.4	14.0	52.7	23.70	11.1	36.5	55.6	58.	14.2	366.0	86.4	86	5	9	Sand
P3 – Turbic Leptic Umbric Skeletic Cryosol (Arenic Humic)																									
A1	0-10	5.1	4.3	222.9	123	162.8	2.1	1.4	1.5	16.1	4.5	6.1	20.6	22.1	25.5	17.2	5.9	3.3	15.2	588	1.4	94	3	3	Sand
B	10-20	5.7	4.4	248.4	103	148.8	2.5	1.5	0.8	13.8	4.9	5.7	18.6	26.2	15.3	11.7	6.2	4.5	23.0	756.1	1.6	94	3	3	Sand
P4 – Turbic Leptic Cryosol (Arenic, Humic)																									
A	0-10	5.0	4.2	239.5	113	124.4	1.6	0.5	1.1	11.4	3.0	4.1	14.4	20.8	26.8	8.0	8.4	3.1	13.5	309.1	2.6	77	11	12	Sandy loam
C	10-20	5.4	4.6	429.1	252	254.5	2.8	1.3	0.6	10.5	5.9	6.5	16.4	36.0	9.1	6.8	7.8	8.8	19.5	609.4	3.4	91.2	5.4	3.4	Sand
P5 – Turbic Leptic Cryosol (Arenic Humic Ornithic)																									
A	0-10	5.0	4.4	260.5	103	108.7	1.8	0.8	0.8	12.9	3.4	4.3	16.3	21.1	20.4	9.7	25.5	3.8	21.7	572.1	1.7	85.1	2.4	2.5	Sand
C	10-20	5.9	4.6	432.6	252	274.6	2.7	1.3	0.3	10.8	5.8	6.1	16.6	35.2	4.7	7.1	7.0	8.9	15.4	648.4	3.1	60.6	31.7	4.5	Sand
P6 - Turbic Leptic Cryosol (Arenic)																									
A/B	0-5/10	5.9	4.9	685.1	72	98.7	13.7	3.7	0	1.0	18.0	18.0	19.0	94.8	0	0.7	35.7	7.1	40.9	340.6	3.4	93.4	3.1	3.5	Sand
B2	5/10-15/20	5.2	4.7	1391.4	130	179.9	15.8	3.1	0	1.6	20.0	20.0	21.6	92.6	0	1.9	14.5	17.3	20.3	428.6	12.2	88.8	7.1	4.1	Sand
C	15/20-30	5.7	4.2	1465.9	77	91.6	21.8	3.9	0	0.8	26.4	26.4	27.2	97.1	0	0.5	31.4	21.9	36.6	336.6	12.9	83.0	10.0	7.0	Loamy sand
P7 – Turbic Leptic Umbric Cryosol (Arenic Humic)																									
A	0-7	4.7	4.3	597.8	110	139.8	0.9	0.2	1.2	17.7	2.06	3.3	19.7	10.4	38.1	11.1	12.5	3.6	6.6	878.5	1.9	94.1	3	2.9	Sand
B	7-14	4.9	4.4	804.9	165	156.8	0.5	0.1	1.3	17.4	1.73	3.1	19.1	9.0	44.2	6.1	8.8	17.2	8.0	697.5	3.0	87.7	7.1	5.2	Sand
P8 – Turbic Leptic Umbric Cryosol (Arenic Humic)																									
A	0-10	5.4	4.6	432.6	105	132.8	1.7	1.1	0.8	10.1	3.65	4.5	13.7	26.5	19.4	5.8	11.6	4.3	30.2	740.1	0.9	96.9	1.5	1.7	Sand
B	10-25	5.2	4.8	452.1	69	123.7	2.4	1.4	0.2	10.0	4.61	4.8	14.6	31.6	4.2	5.8	10.9	11.7	16.3	547.8	5.4	94.5	3.4	2.2	Sand
C	25-37+	5.1	3.6	479.5	51	118.3	1.9	1.8	0.3	9.6	4.39	4.7	13.9	31.3	6.5	4.2	8.83	14.2	17.5	425.2	6.8	92.0	4.0	3.0	Sand
P9 – Turbic Reductaquic Leptic Mollic Cryosol (Arenic Humic)																									
A	0-10	5.2	4.7	334.6	333	334.8	5.2	1.5	0	3.9	9.07	9.0	12.9	69.9	0	4.2	24.6	10.3	29.1	661.2	6.8	96.0	2.0	2.0	Sand
B	10-20	5.7	4.4	389.4	97.0	137.8	7.3	1.9	0	4.3	10.0	10.0	14.3	70.0	0	4.9	15.2	6.3	21.7	545.6	2.1	96.0	2.0	2.0	Sand
C	20-25+	5.9	4.6	482.8	104	140.8	7.8	1.8	0	4.5	10.5	10.5	15.0	70.0	0	3.9	13.4	8.7	21.0	65.6	2.3	96.0	2.0	2.0	Sand

Table II. Continuation.

Horizon	Depth (cm)	pH		P	K	Na	Ca^{2+}	Mg^{2+}	Al^{+3}	H + Al	BS	CECeff	CECT	PSB	Al sat	OM	P-Rem	Cu	Mn	Fe	Zn	Sand	Silt	Clay	Texture
		H_2O	KCl	-------- mg/dm³--------			----------cmol$_c$/kg----------							%		dag/kg	mg/L	mg/dm³				%			
P10- Turbic Cryosol (Dystric Arenic Ornithic)																									
C1	0-25	5.4	4.7	2184.2	97	235.1	8.1	3.7	0	6.1	13.1	13.1	19.2	68.2	0	4.9	11.6	7.8	31.5	643.1	0.6				
C2	25-40	5.7	4.8	1753.9	86	209.1	7.5	2.2	0	7.3	10.9	10.9	18.2	60.0	0	3.6	10.3	8.3	33.8	795.7	0.8				
C3	40-60	5.1	4.9	315.3	68	75.6	1.5	0.7	1.4	11.6	2.8	4.2	14.4	19.6	34.1	1.8	21.4	7.9	32.1	871.8	0.7	96.1	1.4	2.4	Sand
C4	60-80+	6.0	4.7	585.9	73	86.5	2.8	0.4	0	6.9	3.8	3.8	10.7	35.9	0	1.2	23.5	7.3	21.7	461.0	1.9	75.7	16	8.3	Sandy loam
P11 - Turbic Leptic Cryosol (Arenic Humic)																									
A	0-8/12	5.1	4.3	183.4	62	120.7	0.9	0.2	0.49	5.8	1.8	2.3	7.6	24.3	20.9	4.2	15.3	4.9	19.0	371.1	2.2	97.1	1.2	1.6	Sand
B1	8/12-18/22	6.0	4.9	1244.4	118	174.3	3.5	1.1	0	7.1	5.7	5.7	12.8	44.5	0	7.8	5.2	30.3	20.3	351.4	24.4	87.9	9.1	3.0	Sand
B2	18/22-28	5.9	4.4	9638.6	66	123.7	1.4	0.4	0.1	5.6	2.53	2.6	8.1	31.1	3.8	5.8	7.0	11.3	25.1	489.1	6.4	94.8	3.1	2.1	Sand
P12 - Skeletic Leptosol (Arenic Gelic Ornithic)																									
Guano	0-2	7.8	8.6	8483.6	3741	4927.5	7.6	8.5	0	0.17	47.1	47.1	47.3	99.6	0	0.1	234.5	11.1	10.2	638.2	4.7				
C1	2-12	7.1	8.6	8951.1	3595	4116.1	10.9	8.4	0.2	0.43	46.4	46.6	46.8	99.8	0.5	0.1	219.3	14.5	14.8	691.5	5.1				
C2	12-23	4.9	8.2	8356.4	3266	3964.2	6.1	8.5	0.6	1.15	33.1	33.8	34.3	96.6	1.8	0	166.2	12.7	26.3	746.3	7.2				
C3	23-30	4.4	8.1	7682.2	3348	3699.8	6.4	7.3	1.5	2.66	38.4	40.0	41.1	93.5	3.9	0	145.0	11.3	19.3	731.4	8.4				
P13- Eutric Skeletic Leptosol (Arenic Gelic)																									
R	0-15	5.7	6.3	1721.5	754	1964.2	8.2	4.6	0	0.81	22.8	22.8	23.7	96.5	0	1.4	83.1	12.5	6.2	462.9	8.2				
P14- Skeletic Leptosol (Arenic Gelic Ornithic)																									
A	0-6	5.5	4.5	1227.6	77	118.7	0.8	0.2	0.4	7.6	1.8	2.2	9.46	19.7	17.3	2.9	24.5	10.7	9.7	660.2	9.3	95.5	2.7	2.0	Sand
B	6-23	5.4	4.1	779.0	67	119.7	0.8	0.2	0.2	6.4	1.7	2.1	8.10	21.0	18.7	1.6	19.5	6.8	18.8	507.6	6.7	94.9	2.8	2.3	Sand
C	23-27+	5.1	3.8	552.9	163	269.2	0.6	0.1	0.1	1.15	2.3	2.4	3.49	67.0	7.64	0.7	43.70	4.1	18.5	326.1	2.4				
P15- Turbic Skeletic Cryosol (Arenic Eutric Patterned)																									
A	0-7	6.7	5.0	64.1	121	237.7	1.6	0.9	0	1.3	3.9	3.9	5.2	75.1	0	0.3	32.5	5.4	23.8	346.4	2.8	82	13.6	4.4	Loamy sand
B1	7-15	7.2	4.2	4.2	115	247.7	3.1	1.7	0	1.3	6.2	6.2	7.5	82.8	0	0.6	23.1	4.7	27.3	350.5	4.1	71.6	23.9	4.5	Loam
B2	15-25	7.0	4.3	982.3	140	317.4	5.1	3.1	0	2.1	9.9	9.9	12.0	82.5	0	1.6	16.6	19.0	50.8	230.1	32.2	56.1	33.7	10.2	Sandy loam
C	25-100	6.9	4.7	1112.11	109	227.8	3.9	1.9	0	2.3	7.1	7.1	9.4	75.6	0	0.3	20.8	20.5	38.9	318.1	24.8	71	21	9	Sandy loam
Cg	100+	7.2	4.8	1174.4	95	205.1	3.7	1.7	0	2.0	6.6	6.6	8.59	76.7	0	1.3	23.2	22.3	39.8	329.2	25.5	77	16	7	Sandy loam
P16 - Eutric Leptosol (arenic Gelic)																									
A	0-10	5.1	4.2	5893.4	192	188.5	4.7	0.5	4.1	1.1	6.6	10.7	7.7	85.0	38.3	1.83	141.1	17.9	23.6	261.6	11.8				
B1	10-15	4.0	4.5	4056.4	189	151.3	3.0	0.2	3.3	41.1	4.4	7.7	45.5	9.7	42.6	6.72	46.2	28.1	3.6	289.2	16.7	57.4	25.3	17.3	Sandy loam

Table II. Continuation.

Horizon	Depth (cm)	pH		P	K	Na	Ca^{2+}	Mg^{2+}	Al^{+3}	H + Al	BS	CECeff	CECT	PSB	Al sat	OM	P-Rem	Cu	Mn	Fe	Zn	Sand	Silt	Clay	Texture
		H_2O	KCl	-------- mg/dm³--------			----------cmol$_c$/kg----------							%		dag/kg	mg/L	mg/dm³				%			
B2	15-20	3.7	4.1	2929.2	195	124.4	1.5	0.1	2.7	43.7	2.7	5.4	46.4	5.8	50.1	4.7	55.3	21.8	2.4	337.1	5.8	62.2	27.3	10.5	Sandy loam
2B3	20-43	3.8	4.2	2469.6	150	70.6	0.7	0.1	2.4	26.4	1.5	3.9	27.9	5.6	60.5	3.02	53.6	10.4	1.0	288.4	1.7	87.3	9.8	2.9	Sand
P17- Skeletic Leptosol (Arenic Gelic)																									
C1	0-20	5.7	4.9	1861.5	68	79.5	2.46	0.5	0.68	13.9	3.4	4.16	17.3	20.0	16.3	2.6	41.9	13.7	10.2	371.1	2.4				
C2	70-100	5.0	4.3	1643.8	61	77.6	1.8	0.3	0.5	7.7	2.6	3.2	10.37	25.7	15.5	2.2	44.4	15.4	10.2	492.8	19.6	98.3	0.6	1.1	Sand
P18- Eutric Leptosol (Siltic Gelic)																									
A	0-7	5.1	4.4	135.7	122	158.3	1.4	2.3	0	0.51	4.7	4.74	5.25	90.2	0	5.26	32.9	2.14	32.3	375.1	2.66				
B1	7-15	6.3	5.0	81.6	144	204.1	2.46	0.98	0	1.0	4.7	4.70	5.70	82.5	0	0.67	40.6	5.67	35.1	589.4	2.86	74.1	23.7	2.2	Loam
B2	15-25+	6.7	4.5	109.4	200	257.7	2.94	1.14	0	1.2	5.7	5.71	6.91	82.6	0	0.34	37.4	11.7	37.9	451.8	3.68	70.4	26.7	3	Loam
P19- Turbic Umbric Cryosol (Arenic Ornithic)																									
A	0-10	7.1	4.6	294.1	135	113.8	3.96	1.22	0	3.4	6.0	6.02	9.42	63.9	0	4.37	3.2	6.29	7.12	188.5	3.74				
B1	10-25	7.1	4.9	189.7	100	194.2	2.88	1.50	0	4.3	5.4	5.48	9.78	56.0	0	3.02	9.5	8.55	13.8	238.4	3.89	68.7	22.6	8.7	Sandy loam
B2	25-37+	7.2	4.4	520.3	165	197.9	3.99	1.98	0	5.1	7.2	7.25	12.35	58.7	0	3.09	9.8	13.5	8.8	394.0	6.74	55.1	34.8	10.1	Sandy loam
P20- Skeletic Leptosol (Arenic Gelic)																									
A/C	0-15	4.2	4.3	357.1	161	83.7	4.5	3.3	1.9	2.6	8.5	10.5	11.1	76.7	18.4	2.8	10.2	27.4	13.6	285.6	3.6				
C	15-25	4.4	4.6	388.5	192	88.1	3.2	2.4	1.8	2.9	6.3	8.3	9.4	69.2	21.7	1.75	9.2	22.1	13.9	281.4	4.1				
P21- Turbic Leptic Umbric Skeletic Cryosol (Arenic Humic)																									
A/B1	0-25	4.8	4.3	636.7	139	135.6	1.85	0.59	1.71	19.4	3.3	5.08	22.8	14.78	33.6	6.21	11.5	21.5	3.0	361.6	3.14				
B2/C	25-40+	5.3	4.5	651.1	129	119.7	1.01	0.24	1.56	14.0	2.1	3.66	16.1	13.0	42.6	5.87	14.7	23.0	21.1	368.2	3.57	94.3	2.2	3.5	Sand

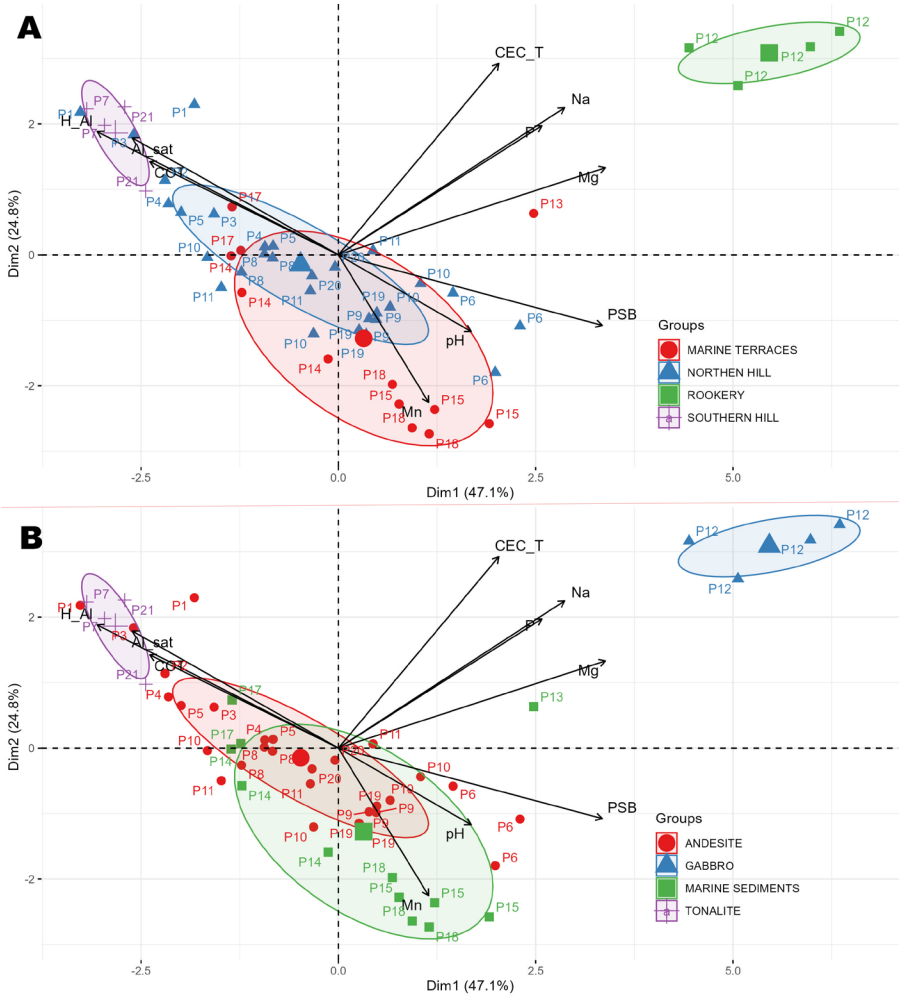

Figure 3. Principal component analysis (PCA) of soil chemical properties from Half Moon Island profiles. a) profiles grouped by landscape units b) profiles grouped by geology types.

content was high, especially in the range of P1-P5, with values above 6 (dag/kg) and up to 36.5 (dag/kg), while low values were recorded in P15 and P18 (0.34 dag/kg). Base sum (BS) and the total cation exchange capacity (CEC_T) varied between the profiles, with values ranging from 1.5 to 47.1 (cmol/dm³) and 3.5 to 52.7 (cmol/dm³), respectively. The soils differed according to the percentage of base saturation (PSB), with P1, P2, P3, P4, P5, P7, P8, P11, P14, P17, and P21 being dystrophic (PSB < 50%) and P6, P9, P12, P15, P18, P19, and P20 being eutrophic (PSB > 50%).

Soil chemical pattern

Principal component analysis (PCA) revealed a high variability of soil chemical properties in the analyzed profiles on Half Moon Island (Figures 3 and 4). The first two axes of the PCA explained 71.9% of the variability in the soil profiles. Thus, the first axis (47.1%) was positively correlated with magnesium (Mg, r = 0.89), base saturation (BS, r = 0.88), and sodium (Na, r = 0.75), and negatively correlated with potential acidity (H+Al, r = -0.80), aluminum saturation (Al sat, r = -0.68), and organic carbon (COT, r = -0.63). The second axis of the PCA (24.8%) is positively correlated with the total cation exchange capacity (CEC_T, r = 0.77).

Profile P12 is located in an active penguin rookery and formed an isolated group from the other profiles due to its distinct and unique chemical characteristics, exhibiting

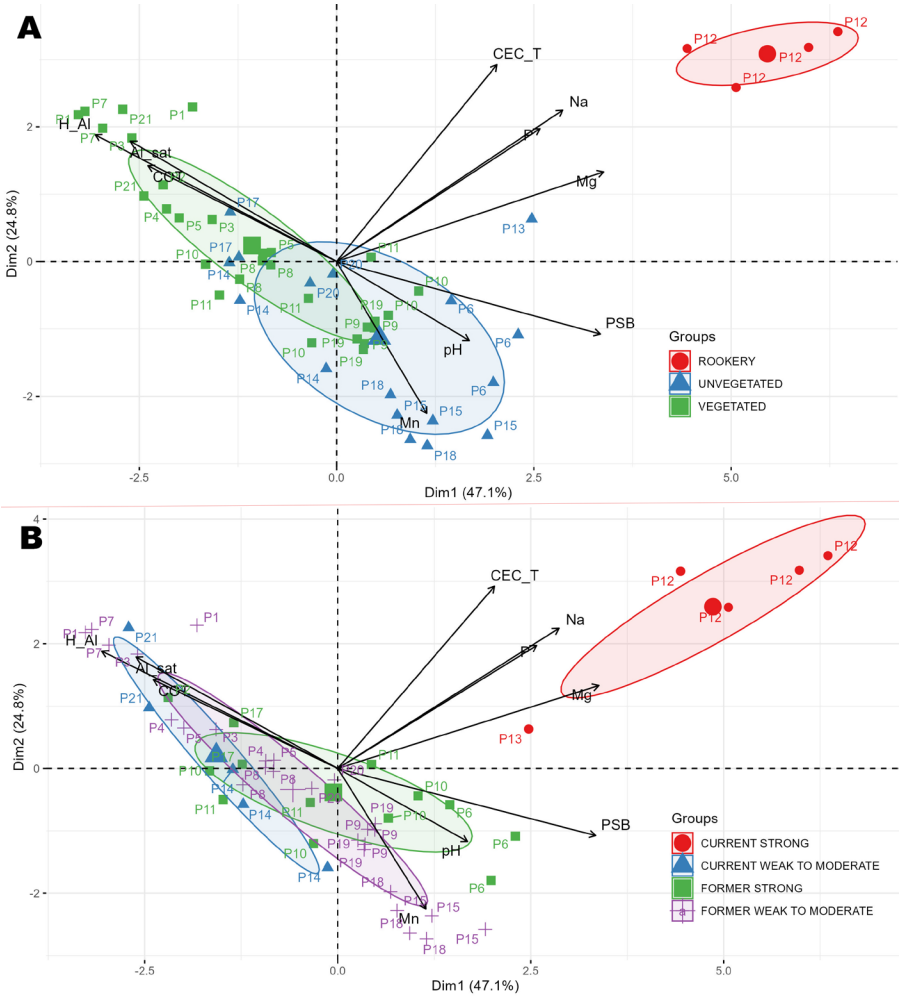

Figure 4. Principal component analysis (PCA) of soil chemical properties from Half Moon Island profiles. a) profiles grouped by vegetation b) profiles grouped by degrees of ornithogenesis.

eutrophic soils, very high levels of phosphorus (P) and sodium (Na), and high values of CEC_T. In addition, due to the intense activity and trampling by penguins, vegetation cannot develop, and the gabbro geology differs from the rest of the island's sites.

In the PCA of the landscape units (Figure 3a), the profiles were grouped into four clusters: marine terraces, Northern Hill, Penguin rookery, and Southern Hill. Profiles P7 and P21 in La Morenita (Southern Hill) were grouped together because they had high potential acidity (H + Al) and similar values for soil organic carbon content (COT) and aluminum saturation (Al sat). The profiles in the marine terraces (P13, P14, P15, P17, and P18) show similar values for micronutrients, such as manganese (Mn), which increase with depth, and low organic matter content which decreases with the depth of the profiles. The profiles in the Northern Hills (Xenia P1, P2, P3, P8, P9, P10, P11, P19, P20, and Gabriel P4, P5, and P6) were grouped together and show high values of organic matter (OM).

In the PCA of the geology of Half Moon Island (Figure 3b), the profiles were grouped into four clusters: three geological formations (andesite, gabbro, and tonalite), and the marine sediments that make up the present beaches. The distribution of the groups among the geological types reflects the distribution among the landscape units. Gabbro rock is restricted to Baliza Point, and only occur in P12. La Morenita

Hill is predominantly composed of tonalitic rocks and hosts the P7 and P21 profiles. In contrast, Xenia and Gabriel Hills (to the North) are predominantly andesite and host the P1, P2, P3, P8, P9, P10, P11, P19 and P20 profiles, as well as the P4, P5, P6 profiles.

In the PCA of the vegetation (Figure 4a), the profiles were divided into three groups: vegetated, unvegetated, and the currently active penguin rookery (P12). The vegetated profiles (P1, P2, P3, P4, P5, P7, P8, P9, P10, P11, and P20) are covered with mosses or lichens and/or mixed communities of both. The vegetated areas are mainly located in the higher parts, of the Xenia, Gabriel, and La Morenita Hills. The unvegetated profiles from the higher elevations (P6 and P20) are located in stone stripes, where constant cryoturbation prevents the establishment of vegetation.

The PCA of ornithogenesis revealed four different degrees of ornithogenic influence on Half Moon Island (Figure 4b). The classification was based on the observation of the presence of flying birds and penguins at the sampled sites and on the phosphorus (P) content, analyzing all horizons of the sampled profiles. Current strong (P12 and P13): profiles located in and around the currently active penguin rookery, respectively. Current weak to moderate: Encompassing P14, located near a currently active penguin rookery at Baliza Point, and P21 near skua nests on La Morenita Hill. Former strong (P2, P6, P10, P11, and P17): occur in the upper areas, especially on the upper platforms and slopes of Xenia and Gabriel Hills, which are no longer accessible to penguins. Former weak to moderate: Profiles located on present-day beaches (P18) and uplifted marine terraces (P15) show a weak ornithogenic influence in the surface horizons, with a tendency towards an increased influence in the deeper horizons. P7, classified with a moderate degree of influence, is located on debris slopes and cones on the ascent of La Morenita, displaying a similar trend of increasing phosphorus (P) content with depth. This pattern is also observed in profiles P1, P3, P4, P5, P8, P9, P19, and P20, which are located in the higher areas of Xenia and Gabriel Hills.

Soil map classification

The digital soil mapping, which combines landscape aspects with the described soil types, resulted in nine different soil classes (Figure 5). These classes had different percentages of coverage on the ice-free areas, with the class "Lithic Gelorthent + Typic Gelorthent + beach gravels (Skeletic Leptic Regosol + Skeletic Regosol)" covering the most of the island, with 32.4%, followed by "Typic Gelorthent (Skeletic Regosol)" with 18.3%, both of which are mainly located in areas of marine landforms and deposits where present-day and Holocene beaches occur. At 12.4%, "Lithic Umbriturbels + Lithic Aquiturbels (Umbric Leptic Cryosol + Reductaquic Leptic Cryosol)" covers most of the upper platforms and scarps, which also include periglacial and nival landforms and deposits, as well as patterned ground, nivation niches, and solifluction lobes. The soils classified as "Lithic Gelorthent (Skeletic Leptosol)" account for 11.2% and occur mainly on hill slopes in areas with periglacial and nival landforms and deposits, such as debris slopes and cones. With a total of 10.5%, the soils "Typic Psammoturbels + Lithic Umbriturbels (Turbic Cryosol (Arenic) + Umbric Leptic Cryosol)" occupied the areas above 70 m a.s.l. of Hills Gabriel, Xenia, and La Morenita, and above 40 m a.s.l. in Baliza Point. The "Typic Psammoturbels + Lithic Umbriturbels (Turbic Skeletic Cryosol (Arenosol) + Umbric Leptic Cryosol)" soils (in light blue) covered 6.3% of the area and are located on the central tombolo (40 m a.s.l.), which connects the hills in the north with the southern part of the island. The soils

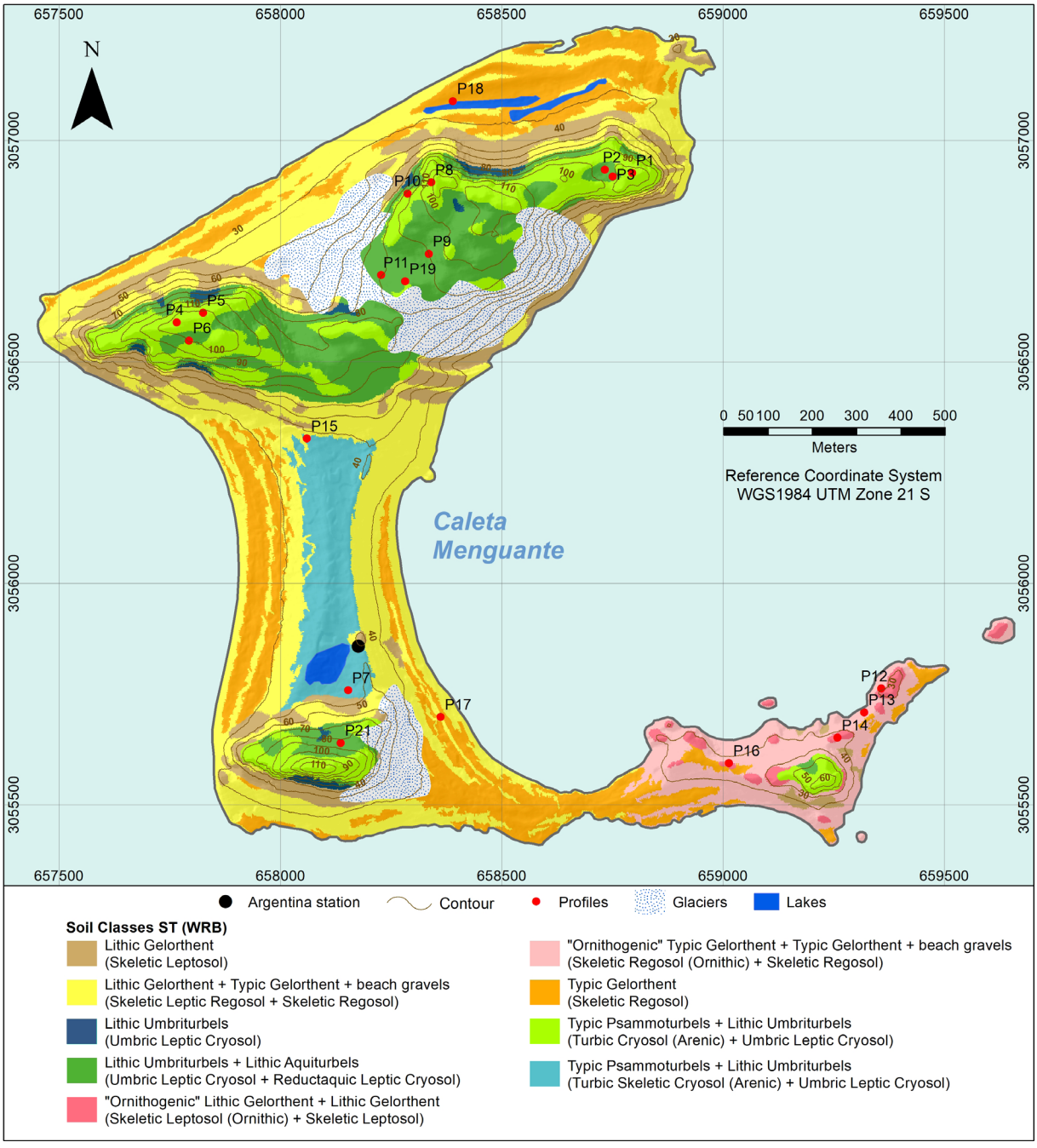

Figure 5. Soil classification map of Half Moon Island, featuring the locations of the 21 sampled profiles.

with the strongest ornithogenic influence are classified as “Ornithogenic Typic Gelorthent + Typic Gelorthent (Skeletic Regosol (Ornithic) + Skeletic Regosol)” and “Ornithogenic Lithic Gelorthent + Lithic Gelorthent (Skeletic Leptosol (Ornithic) + Skeletic Leptosol)” with 6.8% and 0.9% respectively and are restricted to the present-day and Holocene beaches of Baliza Point. Finally, we have the class Lithic Umbriturbels (Umbric Leptic Cryosol), which accounts for 0.8% of the soil coverage on Half Moon Island.

DISCUSSION

Previous studies have shown that Half Moon Island has a clear gradient in terms of relief (Serrano & López-Martínez 1997, López-Martínez et al. 2012), vegetation establishment (Schmitz et al. 2018, 2021), and geology (Smellie et al. 1984). In addition, the soils of HMI are strongly influenced by the intense activity of seabirds that inhabit the island (Esponda et al. 2000), as well as a milder climate compared to continental Antarctica, similar to other islands in the South Shetland archipelago. Our results shed light on the factors for the formation of the islands, their ornithogenic status and the development of vegetation influenced by the geology and geomorphologic evolution of the HMI since the last glacial period (LGM). Before the glacio isostatic uplift, the penguin colonies colonised areas that are now inaccessible to them due to the elevation of the platforms . Since it is a small island and the hills have no current tombolo connections, much of the area was used by penguins for nesting. A strong ornithogenesis can therefore be observed, which is due to the earlier colonisation of these areas, which are now elevated. The current colonisation takes place on current and Holocene beaches to which the penguins have easy access.

According to Massone et al. (1996) the widespread presence of raised geomorphological features of marine origin on HMI allows us to infer its Quaternary evolution, which is closely linkedto glacial and interglacial events. The Quaternary evolution of HMI can be divided into four stages: glacial 1, interglacial, glacial 2 and postglacial, which can be correlatedwith existing regional schemes for the South Shetland Islands. During glacial 1 the island was covered by ice and connected to the other islands. Several marine erosional surfaces which today lie between 100 and 45 m were formed during the interglacial. During the subsequent local glaciation (Late Pleistocene), the ice formed a platform that later controlled the sedimentation of a tombolo. The postglacial period is characterized by a relative decline in sea level, interrupted by three stadial intervals. The first, 9000-7000 years BP, formed a gravel beach at 18 m above sea level and created a tombolo in the central area of the island. The second, during the 13th century, formed gravel beaches at 6 m, and the last (during the 18th century) formed a gravel beach at 3 m which generated another tombolo to the south of the island.

Fretwell et al. (2010) build a polynomial model showing a regional uplift of 18 to 20 m since the formation of the highest beach, equating to a longterm average of 2.8 mm of uplift per year. The change during the Holocene is controlled primarily by variations in glacio-isostacy rather than tectonic activity. The centre of uplift is located in the English Strait between Greenwich Island and Robert Island. The main axis of uplift runs along the axis of the island chain.

Bertola & Isla (1996) describe Half Moon Island's coastline as predominantly composed of gravel beaches with diverse profiles and compositions. The formation and evolution of these beaches are linked to sea level changes during the Holocene, which have been further influenced by contemporary wind and wave dynamics. Fossil beaches are the result of episodic events that led to the accumulation of gravel at higher-than-usual levels. The net gravel transport and volumetric balance for the island's entire shoreline were calculated, showing an annual transport of 13,200 m^3 of gravel. This transport is affected by wave action, coastal and tidal currents, differences in pavement compaction, and the residence time of icebergs and pack ice. Beaches in the southern part of the island exhibit less dynamic behavior than

those in the northern part. Material movement around the island follows a clockwise direction (Mekhova et al. 2023). High beach levels are explained not only by sea level fluctuations but also by neotectonic activity, tsunamis caused by underwater slumps, glacier collapses, and "jökulhlaups" associated with the nearby active volcano of Deception Island.

Serrano & López-Martínez (1997) highlight marine landforms as the defining features of the island. The island's current configuration resulted from the merging of three small islands during the Quaternary period, connected by two tombolos. They identify three primary groups of marine landforms and deposits: upper platforms (70-90 m), middle platforms (approximately 40 m), and lower raised beaches (less than 18 m). The upper and middle platforms date back to the pre-Holocene, while the lower raised beaches are from the Holocene. Glacial activity has modified the upper areas, and periglacial landforms have recently formed in deglaciated regions. Two residual ice masses, remnants of a former glacial dome situated on the platform between Xenia and Gabriel Hills, remain. This glacier left deposits, tills, and moraines, probably from the Little Ice Age readvance.

Periglacial landforms and processes are currently significant, with both active and inherited features. Seven types of periglacial landforms have been identified on beaches and marine platforms, all located above 10 m a.s.l., with patterned ground extensively developed above 18 m a.s.l. Currently, periglacial processes have reduced activity. The island's geomorphological evolution can be described in several phases. Initially, general erosion shaped the upper platforms. This was followed by further erosion, resulting in the existence of several small islands, all occurring in the pre-Holocene. During the Holocene, an accumulation phase led to the formation of the tombolo connecting Xenia-Gabriel and La Morenita. Subsequent uplift created up to 14 levels of raised beaches and formed the tombolo between La Morenita and Baliza Point.

Based on regional chronology by other researchers, the accumulation phase is estimated to have occurred 5000-6000 years BP, and the Baliza Point connection around 1900-2200 years BP. In recent times, glaciers in the upper areas have advanced, occurring 800-500 years BP, along with increased periglacial activity in the lower areas (Fretwell et al. 2010). During the Little Ice Age, the Equilibrium Line Altitude (ELA) was at 70-90 m a.s.l., but it has since risen above 90 m. Currently, glaciers are retreating from their previous positions.

CONCLUSIONS

The landscape evolution of Half Moon Island has played a significant role in soil formation and ornithogenesis, driving the establishment of plant communities. Before the glacio-isostatic uplift, penguin colonies inhabited high areas, now inaccessible due to the glacial rebound. This paleo-occupation resulted in pronounced ornithogenesis in these elevated regions, and greater vegetation growth.

On Half Moon Island, we identified four degrees of ornithogenic influence: current strong: Found in and around the active penguin rookery; current weak to moderate: located at the surroundings of the active penguin rookery; former strong: paleo penguin rookeries at the upper areas, particularly Xenia and Gabriel Hills; former weak to moderate: located on present-day beaches and uplifted marine terraces (Late Holocene).

Nine different soil classes occur on this tiny island, each one possessing unique characteristics and distribution across Half Moon Island. They include Lithic Gelorthent, Typic

Gelorthent, Skeletic Leptic Regosol, Skeletic Regosol, Umbric Leptic Cryosol, Reductaquic Leptic Cryosol, Skeletic Leptosol, Turbic Cryosol, Umbric Leptic Cryosol, and Arenic Leptosol.

The high pedodiversity results from the complex geological and ecological history of Half Moon Island, showcasing the intricate interplay between natural processes, ornithogenic activity, and environmental factors that shaped the Maritime Antarctica.

Acknowledgments

We acknowledge the Conselho Nacional de Desenvolvimento Científico e Tecnológico (CNPq) for the financial support to project no. 440910/2023-4 (Permaclima) and for the first author's DTI grant no. 381136/2024-8 (CNPq). We thank the Brazilian Navy and the Oceanographic Support Ship Ary Rongel for their logistical support during expeditions to Antarctica. We also extend our gratitude to the Brazilian Antarctic Program (PROANTAR) and the Interministerial Secretariat for Marine Resources (SECIRM) for their financial and logistical support. We appreciate the welcome and support provided by Base Argentina Camara during the fieldwork. This work was a contribution from the INCT-Criosfera-TERRANTAR and INCT-APA groups.

REFERENCES

BERTOLA G & ISLA F. 1996. Dynamics and evolution of gravel beaches in Half Moon Island, South Shetland, Antarctica. Revista de la Asociacion Geologica Argentina 48(2): 15-19.

BOCKHEIM JG, BALKS MR & MCLEOD M. 2006. ANTPAS Guide for Describing, Sampling, Analyzing, and Classifying Soils of the Antarctic Region, ANTPAS, p. 1-12.

CAMPBELL IB & CLARIDGE GGC. 1987. Antarctica: Soils, weathering processes and environment. Elsevier, Amsterdam, p. 368 p.

CONVEY P, GIBSON JAE, HILLENBRAND CD, HODGSON DA, PUGH PJA, SMELLIE JL & STEVENS MI. 2008. Antarctic terrestrial life – challenging the history of the frozen continent? Biol Rev 83: 103-117. doi:10.1111/j.1469-185X.2008.00034.x.

DAHER M, SCHAEFER CEGR, THOMAZINI A, NETO EL, SOUZA CD & LOPES DV. 2019. Ornithogenic soils on basalts from maritime Antarctica. Catena 173: 367-374. https://doi.org/10.1016/j.catena.2018.10.028.

ESPONDA CMG, CORIA NR & MONTALTI D. 2000. Breeding birds at Halfmoon Island, South Shetland Islands, Antarctica, 1995/96. Marine Ornithol 28 59-62.

FERRARI FR, SCHAEFER CEGR, PEREIRA AB, THOMAZINI A, SCHMITZ D & FRANCELINO MR. 2021. Coupled soil-vegetation changes along a topographic gradiente on King George Island, maritime Antarctica. Catena 198: 105038. https://doi.org/10.1016/j.catena.2020.105038.

FRANCELINO MR, SCHAEFER CEGR, SIMAS FNB, FILHO EIF, SOUZA JJLL & COSTA LM. 2011. Geomorphology and soils distribution under paraglacial conditions in an ice-free area of Admiralty Bay, King George Island, Antarctica. Catena 85: 194-204. https://doi.org/10.1016/j.catena.2010.12.007.

FRETWELL PT, HODGSON DA, WATCHAM EP, BENTLEY MJ & ROBERTS SJ. 2010. Holocene isostatic uplift of the South Shetland Islands, Antarctic Peninsula, modelled from raised beaches. Quat Sci Rev 29: 1880-1893.

GEE GW & BAUDER JW. 1986. Particle-size analysis. In: Klute A (Ed), Methods of Soil Analysis. Part 1: Physical and Mineralogical Methods. Soil Science Society of America, Madison, p. 383-412.

HUSSON F, JOSSE J, LE S & MAZET J. 2017. "FactoMineR" package Multivariate: Exploratory Data Analysis and Data Mining. http://CRAN.R-project.org/package=FactoMineR. RStudio package version 1.0.14.

IUSS WORKING GROUP WRB. 2015. World Reference Base for Soil Resources 2014, update 2015 International soil classification system for naming soils and creating legends for soil maps. World Soil Resources reports no. 106. FAO, Rome.

LOPES DV, SCHAEFER CEGR, SOUZA JJLL, OLIVEIRA FS, SIMAS FNB, DAYER M & GJORUP DF. 2019. Concretionary horizons, unusual pedogenetic processes and features of sulfate affected soils from Antarctica. Geoderma 347: 13-24. https://doi.org/10.1016/j.geoderma.2019.03.024.

LÓPEZ-MARTÍNEZ J, SERRANO E, SCHMID T, MINK S & LINÉS C. 2012. Periglacial processes and landforms in the South Shetland Islands (northern Antarctic Peninsula region). Geomorph 155-156: 62-79. doi:10.1016/j.geomorph.2011.12.018.

MASSONE HE, MARTINEZ GA & DEL RIO JL. 1996. Quaternary glaciation of isla Media Luna, South Shetland Islands, Antarctica. Revista de la Asociacion Geologica Argentina 51(4): 313-320.

MEKHOVAA OS, SMIRNOVAA DA, MOROZOVA EG, OSTROUMOVAA SA, & FREYA DI. 2023. Internal Waves near Half Moon Island, South Shetland Islands. Oceanology 63(4): 486-496.

MICHEL RFM, SCHAEFER CEGR, DIAS L, SIMAS FNB, BENITES V & MENDONÇA ES. 2006. Ornithogenic Gelisols (Cryosols) from Maritime Antarctica: pedogenesis, vegetation and carbon studies. Soil Sci Soc Am J 70: 1370-1376.

MYRCHA A & TATUR A. 1991. Ecological role of the current and abandoned penguin rookeries in the land environment of the maritime Antarctic. Polish Polar Research 12 (1): 3-24.

PEREIRA TTC, SCHAEFER CEGR, KER JC, ALMEIDA CC, ALMEIDA ICC & PEREIRA AB. 2013. Genesis, mineralogy and ecological significance of ornithogenic soils from a semi-desert polar landscape at Hope Bay, Antarctic Peninsula. Geoderma 209-210: 98-109.

PERFETTI-BOLAÑO A, MORENO L, URRUTIA R, ARANEDA A & BARRA R. 2018. Influence of Pygoscelis Penguin Colonies on Cu and Pb Concentrations in Soils on the Ardley Peninsula, Maritime Antarctica. Water Air Soil Pollut 229: 390. https://doi.org/10.1007/s11270-018-4042-4.

POGGERE GC, MELO VF, FRANCELINO MR, SCHAEFER CE & SIMAS FN. 2016. Characterization of products of the early stages of pedogenesis in ornithogenic soil from Maritime Antarctica. Eur J Soil Sci 67: 70-78.

QGIS. 2024. Qgis.org. QGIS Geographic Information System. QGIS Association. http://www.qgis.org.

R CORE TEAM. 2023. R: A language and environment for statistical computing. R Foundation for Statistical Computing, Vienna, Austria. URL http://www.R- project.org/.

RODRIGUES WF, SOARES FS, SCHAEFER CEGR, LEITE MGP & PAVINATO PS. 2021. Phosphatization under birds' activity: Ornithogenesis at diferente scales on Antarctic Soilscapes. Geoderma 391: 114950. https://doi.org/10.1016/j.geoderma.2021.114950.

SACRAMENTO IF, SCHAEFER CEGR, SIQUEIRA RG, CORRÊA GR, PUTZKE J, MICHEL RFM & FRANCELINO MR. 2023. Ornithogenesis and soil-landscape interplays at northern Harmony Point, Nelson Island, Maritime Antarctica. An Acad Bras Cienc 95: e20230722 DOI 10.1590/0001-3765202320230722.

SANTAMANS AC, BOLUDA R, PICAZO A, GIL C, RAMOS-MIRAS J, TEJEDO P, PERTIERRA LR, BENAYAS J & CAMACHO A. 2017. Soil features in rookeries of Antarctic penguins reveal sea to land biotransport of chemical pollutants. PLoS ONE 12(8): e0181901. https://doi.org/10.1371/journal.pone.0181901.

SANTORA JA, LARUE MA & AINLEY DG. 2020. Geographic structuring of Antarctic penguin populations. Global Ecol Biogeogr 1-13. DOI: 10.1111/geb.13144.

SCHAEFER CEGR, FRANCELINO MR, PEREIRA AB, MICHEL RFM, SCHMITZ D, SACRAMENTO IF, RODRIGUES WF & DE MIRANDA CO. 2023. Thermal monitoring of a Cryosol in a high marine terrace (Half Moon Island, Maritime Antarctica). An Acad Bras Cienc 95: e20210692. https://doi.org/10.1590/0001-3765202320210692.

SCHAEFER CEGR, PEREIRA TTC, ALMEIDA ICC, MICHEL RFM, CORRÊA GR, FIGUEIREDO LPS & KER JC. 2017. Penguin activity modify the thermal regime of active layer in Antarctica: a case study from Hope Bay. Catena 149: 582-591.

SCHAEFER CEGR, PEREIRA TTC, KER JC, ALMEIDA ICC, SIMAS FNB, SOARES DE OLIVEIRA F, CORRÊA GR & VIEIRA G. 2015. Soils and Landforms at Hope Bay, Antarctic Peninsula: Formation, Classification, Distribution, and Relationships. Soil Sci Soc Am J 79: 175-184. https://doi.org/10.2136/sssaj2014.06.0266.

SCHMITZ D, PUTZKE J, ALBUQUERQUE MP DE, SCHÜNNEMAN AL, VIEIRA FCB, VICTORIA FC & PEREIRA AB. 2018. Description of plants communities from Half Moon Island, Antarctica. Polar Res 37(1): 1523663.

SCHMITZ D, SCHAEFER CEGR, PUTZKE J, FRANCELINO MR, FERRARI FR, CORRÊA GR & VILLA PM. 2020. How does the pedoenvironmental gradient shape non-vascular species assemblages and community structures in Maritime Antarctica? Ecol Indic 108: 105726.

SCHMITZ D, VILLA PM, MICHEL RFM, PUTZKE J, PEREIRA AB & SCHAEFER CEGR. 2021. Species composition, diversity and coverage pattern of associated communities of mosses-lichens along a pedoenvironmental gradient in Maritime Antarctica. An Acad Bras Cienc 94: 1-17. https://doi.org/10.1590/0001- 3765202120200094.

SERRANO E & LÓPEZ-MARTINEZ. 1997. Evolución de las formas del relieve y los depósitos superficiales cuaternarios em la Isla Media Luna, Islas Shetland del Sur. Bol R Soc Esp Hist Nat (Sec. Geol.) 93(1-4): 207-218.

SIMAS FNB, SCHAEFER CEGR, MELO VF, ALBUQUERQUE-FILHO MR, MICHEL RFM, PEREIRA VV, GOMES MRM & DA COSTA LM. 2007. Ornithogenic Cryosols from Maritime Antarctica: phosphatization as a soil forming process. Geoderma 138: 191-203.

SMELLIE JL, PANKHURST RJ, THOMSON MRA & DAVIES RES. 1984. The geology of the South Shetland Islands: VI Stratigraphy. Geochesmistry and Evolution. Brit Antarct Surv 87: 1-86.

SSS. 2014. Keys to Soil Taxonomy, 12th ed., United States Department of Agriculture, 360 p.

TATUR A, MYRCHA A & NIEGODZISZ J. 1997. Formation of abandoned penguin rookery ecosystems in the maritime Antarctic. Polar Biol 17: 405-417.

TATUR A. 2002. Ornithogenic Ecosystems in the Maritime Antarctic- Formation, development and Disintegration.

TEIXEIRA PC, DONAGEMA GK, FONTANA A & TEIXEIRA WGL. 2017. Manual de métodos de análises de solo. 3ª Edição. Embrapa Solos, Rio de Janeiro, RJ, p. 95-116: 198-397.

How to cite

SCHMITZ D, SIQUEIRA RG, MICHEL RFM, PEREIRA AB, PUTZKE J, FRANCELINO MR & SCHAEFER CEGR. 2024. Pedodiversity and ornithogenesis of a tiny Antarctic Island (Half Moon): landform-geology-vegetation interrelationships. An Acad Bras Cienc 96: e20240581. DOI 10.1590/0001-3765202420240581.

Manuscript received on May 31, 2024;
accepted for publication on September 25, 2024

DANIELA SCHMITZ[1,2,3]
https://orcid.org/0000-0002-3162-2430

RAFAEL G. SIQUEIRA[1,4]
https://orcid.org/0000-0003-2779-136X

ROBERTO F.M. MICHEL[5]
https://orcid.org/0000-0001-5951-4610

ANTONIO B. PEREIRA[6]
https://orcid.org/0000-0003-0368-4594

JAIR PUTZKE[6]
https://orcid.org/0000-0002-9018-9024

MARCIO R. FRANCELINO[1]
https://orcid.org/0000-0001-8837-1372

CARLOS ERNESTO G.R. SCHAEFER[1]
https://orcid.org/0000-0001-7060-1598

[1]Universidade Federal de Viçosa (UFV), Núcleo Terrantar, Departamento de Solos, Vila Gianetti, 8, 36570-075 Viçosa, MG, Brazil

[2]Universidade Federal de Viçosa (UFV), Departamento de Biologia Vegetal, Av. PH Rolfs, s/n, 36570-900 Viçosa, MG, Brazil

[3]ProBioDiversa Brasil, Associação para Conservação da Biodiversidade, Rua Doutor Milton Bandeira, 75, 36570-172 Viçosa, MG, Brazil

[4]Universidade Federal de Viçosa (UFV), Departamento de Geografia, Av. PH Rolfs, s/n, 36570-900 Viçosa, MG, Brazil

[5]Universidade Estadual de Santa Cruz (UESC), Departamento de Ciências Agrárias e Ambientais, Rodovia Jorge Amado, s/n, Km 16, Salobrinho, 45662-900 Ilhéus, BA, Brazil

[6]Universidade Federal do Pampa (UNIPAMPA), Programa de Pós-Graduação em Ciências Biológicas, Rua Aluízio Barros Macedo, s/n, BR 290, Km 423, 97307-020 São Gabriel, RS, Brazil

Correspondence to: **Daniela Schmitz**
E-mail: danni_schmitz@hotmail.com, daniela.schmitz@ufv.br

Author contributions

CEGRS and RFMM designed the study. DS, ABP, JP and RFMM carried out the fieldwork. DS, RGS and RFMM execution of the research, interpreted the results and wrote the first version of the manuscript. RGS produced the maps and assisted with statistical analyses. RFMM collected and classified the soils. CEGRS, ABP and MRF supervised and secured financial resources to conduct this research.